Journal of Functional Foods 25 (2016) 568–578

Available online at www.sciencedirect.com

ScienceDirect

journal homepage: www.elsevier.com/locate/jff

Lepisanthes alata (Malay cherry) leaves are potent inhibitors of starch hydrolases due to proanthocyanidins with high degree of polymerization

Yan Zhang [a], *Adeline Ik Chian Wong* [a], *Ji'en Wu* [a], *Nura Binte Abdul Karim* [b], *Dejian Huang* [a,c,*]

[a] *Food Science and Technology Programme, c/o Department of Chemistry, National University of Singapore, 3 Science Drive 3, Singapore 117543, Singapore*

[b] *Singapore Botanic Gardens, 1 Cluny Road, Singapore 259569, Singapore*

[c] *National University of Singapore (Suzhou) Research Institute, 377 Lin Quan Street, Suzhou Industrial Park, Jiangsu 215123, China*

ARTICLE INFO

Article history:
Received 23 April 2016
Received in revised form 23 June 2016
Accepted 30 June 2016
Available online 14 July 2016

Keywords:
Lepisanthes alata
Proanthocyanidins
α-amylase
α-glucosidase
Inhibition mechanism

ABSTRACT

Type-II diabetes has become a health threat globally. One major challenge for diabetes patients is to control their post-prandial hyperglycaemia, which could be achieved through the inhibition of α-amylase and α-glucosidase. *Lepisanthes alata* (Malay cherry) was discovered as a promising edible plant with high starch hydrolase inhibition activities for corn starch hydrolysis with IC_{50} of its aqueous extracts at 0.77 ± 0.09 μg/mL (for porcine α-amylase) and 10.83 ± 0.67 μg/mL (for rat intestinal α-glucosidase). Proanthocyanidins were identified to be responsible as active compounds. The proanthocyanidin exhibited high degree (mDP at 27) of polymerization and was composed of (epi)catechins and (epi)gallocatechins linked through B-type 4–8 interflavanyl bonds. Inhibition kinetic study revealed that the proanthocyanidins were a mixed noncompetitive inhibitor against α-amylase but competitive inhibitor against α-glucosidase. Our discovery highlighted the potential of the leaves of *L. alata* for use in prevention of post prandial hyperglycaemia.

1. Introduction

Diabetes mellitus is a complex disease affecting patients' daily life and elevating patients' risk of developing other diseases (Wild, Roglic, Green, Sicree, & King, 2004). According to the World Health Organization (WHO), around 422 million people worldwide have diabetes and 90% of them have Type-II diabetes. WHO projected that mortality due to diabetes will more than double between 2016 and 2036 (WHO, 2016). Type-II diabetes is a metabolic disorder in the endocrine system where patients are either insulin-insensitive or insulin-insufficient (Liu, Song, Wang, & Huang, 2011; Mellor, Sathyapalan, Kilpatrick, & Atkin, 2015; Murotomi et al., 2015). These result in a high

* *Corresponding author.* Food Science and Technology Programme, c/o Department of Chemistry, National University of Singapore, 3 Science Drive 3, Singapore 117543, Singapore. Fax: +65 6775 7895.
E-mail address: chmhdj@nus.edu.sg (D. Huang).

Chemical compounds: Epicatechin (PubChem CID: 72276); Catechin (PubChem CID: 9064); Epigallocatechin (PubChem CID: 72277); Gallocatechin (PubChem CID: 65084); Acarbose (PubChem CID: 71312704).

http://dx.doi.org/10.1016/j.jff.2016.06.035
1756-4646/

postprandial spike in blood glucose levels after consumption of foods with high glycaemic index. Postprandial hyperglycaemia is a concern in the management of Type-II diabetes. Alpha-amylase is one of the main enzymes responsible for hydrolysing starch. It is secreted by the pancreas and salivary gland in humans (Nakamura et al., 1984). Inhibition of α-amylase and α-glucosidase is postulated to be a preventive treatment among the available antidiabetic therapeutic methods (Bhandari, Jong-Anurakkun, Hong, & Kawabata, 2008; Clissold & Edwards, 1988; de Camargo, Regitano-d'Arce, Biasoto, & Shahidi, 2016; Holman, Cull, & Turner, 1999; Saito, Sakai, Suzuki, Sekihara, & Yajima, 1998; Toeller, 1994). Currently, oral anti-diabetic drugs belonging to the category of α-glucosidase inhibitors, such as acarbose, miglitol, and voglibose, are available. These drugs work by inhibiting the activity of α-glucosidase, effectively diminishing the spike in blood glucose levels in Type-II diabetic patients. However, long-term use of these drugs promotes detrimental side effects, which include diarrhoea, abdominal cramping, and flatulence (Ma et al., 2015). In the meantime, many natural products and herbal medicines played an important role in treating diabetes in Asia, India, and Africa for centuries. Yet the action principles of the traditional wisdom are not clear and the scientific evidence of their effectiveness remains to be established. In recent years, there is a growing number of research on α-amylase inhibitors in natural products that address postprandial hyperglycaemia but have shown no adverse side effects (Perricone, 2010). Edible plants contain a wide range of secondary metabolites that have diverse bioactivities. To uncover their potentials as good grade inhibitors for mitigating starch digestion rate in our staple foods, which are high in starch, our lab has developed a rapid assay, based on starch turbidity change, for the evaluation of starch hydrolase inhibitors and successfully applied the assay to screen over one hundred food grade traditional herbs for their inhibition activity (Feng et al., 2013; Liu et al., 2011). To extend our survey of the edible plant based starch hydrolase inhibitors, we screened the leaves of about three hundred tropical medicinal plants growing in the Healing Gardens in Singapore Botanic Gardens (data not shown). Our efforts led to the discovery of *L. alata* leaves with high α-amylase inhibition activity, and reported herein are our results on the active compounds in the leaves of this tropical tree.

Proanthocyanidins are polymeric flavan-3-ols existing in natural plants and particularly rich in some fruits and cereals as well as legumes such as peanuts and lentils (Alshikh, de Camargo, & Shahidi, 2015; Chai et al., 2015; de Camargo, Regitano-d'Arce, Gallo, & Shahidi, 2015). Proanthocyanidins are categorized into A type and B type according to linkage sites of their basic units, which means A type is linked by C—C and C—O—C bonds and B type only by C—C bonds (Shahidi & Naczk, 2003). Their different structures are mostly due to the number of hydroxyl groups on aromatic rings and the stereochemistry of the asymmetric carbons of the heterocycle. Although there are different structural proanthocyanidins, some general characteristics including high molecular weights and phenolic properties are shared (Santos-Buelga & Scalbert, 2000). Proanthocyanidins (PACs) are highly structurally diverse and thus PACs from different botanical sources display various biological activities, such as antidiabetic (Nyambe-Silavwe et al., 2015), antioxidant (Shahidi & Ambigaipalan, 2015), antitumoral (Bruyne, Pieters, Deelstra, & Vlietinck, 1999), and antibacterial activities (Bruyne et al., 1999).

Lepisanthes alata, also known as Malay cherry or Johore tree, belongs to the family of Sapindaceae. In South Thailand, young leaves are cooked and eaten as vegetables with a little bit astringent taste and the aril of the ripe fruit with a fairly sweet taste is also edible (Kalsum & Mirfat, 2014; Lim, 2013). Unlike tart cherry (*Prunus cerasus* L.) and sweet cherry (*Prunus avium* L.) with significant attention for their health benefits, there is little research on the bioactive compounds in *L. alata*. In the ageing society, it is important to explore new edible plants as novel source for functional foods. To this end, screened large number of edible plants in tropical areas and found that the aqueous extracts of *L. alata* had high starch hydrolase inhibitory activities. However, to the best of our knowledge, the active compounds of *L. alata* and their inhibitory activities are unclear. Our research on the phytochemicals in this tree uncovers the potential for its use as anti-diabetic food ingredients.

2. Materials and methods

2.1. Materials

Corn starch, α-amylase (type VI-B, from porcine pancreas), α-glucosidase in the form of rat intestine acetone powder, acarbose, methyl thioglycolate, 3,5-dinitrosalicylic acid (DNSA), 2,5-dihydroxybenzoic acid, and gelatin (G-2500 from porcine skin, type A, 300 bloom) were obtained from Sigma-Aldrich (St Louis, MO, USA). Calcium chloride was purchased from Thermo Fisher Scientific Inc. (Waltham, MA, USA). Phosphate buffered saline (ultra-pure grade) was purchased from Vivantis Technologies (Subang Jaya, Selangor, Malaysia). The mature leaves of *L. alata* were sampled from Singapore Botanic Gardens-Healing Garden, Singapore, in November 2013.

2.2. Aqueous extraction of L. alata leaves

L. alata leaves (2.0 kg) with a moisture content of 51.1% were cleaned using deionized water followed by freeze-drying using an advantage benchtop tray lyophilizer (The VirTis Company, Inc., Gardiner, NY, USA). The freeze-dried leaves were then ground to fine powder using a mini blender (DM-6, YOUQI, Changhua, Taiwan) and stored at –20 °C for the subsequent use. The leaf extraction was performed by continuously shaking the *L. alata* leaves powder (200 g) suspended in deionized water (600 mL) on a vortex shaker (Rotamax 120, Heidolph Instruments GmbH & Co.KG, Schwabach, Bavaria, Germany) at 200 rpm and room temperature for 12 h. Afterwards, the slurry was centrifuged (Eppendorf 5810R, Iberica, Madrid, Spain) at 12,074*g* and 4 °C for 10 min. The separated solid was extracted two more times. The aqueous solutions were combined and concentrated at 40 °C using a rotary evaporator (R-200, Büchi Labortechnik AG, Flawil, St. Gallen, Switzerland) to give concentrated crude extracts, and then were lyophilized to powder and stored in a freezer (–20 °C) for further purification of proanthocyanidins.

2.3. Purification of proanthocyanidins

Lyophilized powder was dissolved in deionized water (100 mg/mL) and centrifuged at 12,074*g* and 4 °C for 10 min to get supernatant. The supernatant was filtered through a 0.45 μm Ministar regenerated cellulose (RC) membrane (Sartorius, Göttingen, Lower Saxony, Germany). The obtained filtrate (2 mL) was injected to a cartridge (RediSep® Rf Reversed-phase C18, 130 g silica) connected to a preparative chromatography (C-700, Büchi Labortechnik AG, Flawil, St. Gallen, Switzerland) with a UV detector set at 210 nm. All eluents were auto-collected in 63 continuously numbered glass tubes. The eluent gradients started with 100% deionized water for 5 min (tube no. 1–17), followed by 20% acetonitrile in deionized water for another 5 min (tube no. 18–35), 20–40% acetonitrile from 10–14 min (tube no. 36–49), and 40–100% acetonitrile from 14–18 min (tube no. 50–63) at a constant flow rate of 85 mL/min. Proanthocyanidins were collected in the eluents in no. 23–31 tubes, which were pooled in a round bottom flask and evaporated at 40 °C to remove acetonitrile. All the aforementioned tube numbers were confirmed in our preliminary experiments. The resulting aqueous solution was freeze-dried to give proanthocyanidins.

2.4. Identification of proanthocyanidins using LC-ESI/MS^4

The proanthocyanidins obtained from the leaves of *L. alata* (10 mg) were dissolved in water (1.0 mL) and filtered through a 0.45 μm RC membrane before used as sample for HPLC analysis. Sample (20 μL) was injected into a high-performance liquid chromatography-electrospray ionization mass spectrometry (LC-ESI/MS^4) system with a stationary phase consisting of a Develosil™ diol column (250 × 4.6 mm i.d., 5 μm, Nomura Chemicals, Seto, Aichi Prefecture, Japan) with a 4 × 4 mm guard column filed with the same packing material. The diode array detector was set at 280 nm. The sample was eluted using a solvent gradient consist of 2% acetic acid in acetonitrile (mobile phase A) and acidic aqueous methanol (CH_3OH: H_2O: HOAc, 95:3:2 v/v/v, mobile phase B). Elution programme started with 7% B for 3 min, ramping up to 37.6% B at 60 min, 100% at 63 min and holding for 7 min at a flow rate of 1.0 mL/min at 35 °C. LC-ESI/MS^4 was acquired using a Bruker Amazon ion trap mass spectrometer (Billerica, MA, USA) equipped with a Dionex UltiMate 3000 RS LC system (Bannockburn, IL, USA). The heated capillary and spray voltage were maintained at 250 °C and 4.5 kV, respectively. Nitrogen was operated at 80 psi for sheath gas flow rate and 20 psi for auxiliary gas flow rate. The MS^4 collision gas was helium with collision energy of 30% of the 5 V end-cap maximum tickling voltage. The full scan mass spectra from *m/z* 100–2000 were acquired in both positive and negative ion modes with a scan speed at one scan per second.

2.5. Identification of proanthocyanidins using MALDI-TOF/MS

Matrix-assisted laser desorption/ionization time-of-flight mass spectrometry (MALDI-TOF/MS) identification was carried out on a Brucker microTOF-QII mass spectrometer equipped with delayed extraction and a dinitrogen laser set at 337 nm (Bruker Daltonics, Bremen, Bremen, Germany). The length of one laser pulse was three nanoseconds. The measurements were carried out using the following conditions: positive polarity, linear flight path with 21 kV acceleration voltage, and 100 pulses per spectrum. The sample was dissolved in deionized water (10 mg/mL) and 2,5-dihydroxybenzoic acid was used as the matrix. An aqueous solution was prepared by mixing proanthocyanidins solution (1.0 μL) with saturated aqueous solution of 2,5-dihydroxybenzoic acid (4.0 μL, 20 mg/mL). The resulting solution (5.0 μL) was evaporated and introduced into the spectrophotometer.

2.6. Thiolysis of proanthocyanidins

Oligomeric proanthocyanidins are depolymerized into monomeric proanthocyanidins during thiolysis reaction, which make the further investigation of the major components as well as determination of the sequence of the proanthocyanidins feasible (Wang, Liu, Song, & Huang, 2012). Thiolysis reaction was conducted according to the study of Fu, Loo, Chia, and Huang (2007) with slight modifications. The thiolysis reaction was initiated by mixing 250 μL of proanthocyanidins obtained from the leaves of *L. alata* (2 mg/mL in methanol), 250 μL of acidified methanol (3.3% HCL in methanol, v/v), and 500 μL of methyl thioglycolate (5% in methanol, v/v) in a small glass tube. The glass tube was tightly sealed and heated in an oil bath at 45 °C for 30 min followed by storing at room temperature for 10 h. Afterwards, the components in the thiolysed proanthocyanidins solution were analysed using LC-ESI/MS^4. The analysis was conducted on an analytical reversed-phase C18 Sunfire column (250 mm × 4.6 mm i.d., 5 μm; Waters, Wexford, Wexford, Ireland) and measured at 280 nm using a diode array detector. The binary mobile phases consisted of A (2% acetic acid in deionized water, v/v) and B (methanol), which were delivered in a linear gradient of B from 15 to 80% (v/v) in 45 min at room temperature. The flow rate was set at 1.0 mL/min.

2.7. Protein-proanthocyanidin binding analysis

Protein-proanthocyanidin binding analysis was conducted according to the study of Siebert, Troukhanova, and Lynn (1996). Proanthocyanidins (0.5 mg/mL in deionized water) was blended with an equal volume of gelatin (10 mg/mL in deionized water) in a centrifuge tube. The mixture was shaken on a vortex shaker at 25 °C for 30 min and then centrifuged at 17,000*g* for 10 min at 25 °C. The resulting supernatant was collected for testing its enzymatic inhibitory activity.

2.8. Inhibitory activities against α-amylase and α-glucosidase

The inhibitory activities of *L. alata* leaves extracts and its proanthocyanidins against α-amylase and α-glucosidase were determined using the turbidity measurement according to literature reports (Liu et al., 2011). Sodium phosphate buffer (0.1 M, pH 6.9) was freshly prepared prior to each test and fortified with calcium chloride (40 ppm) (Morris, Fichtel, & Taylor, 2011). Corn starch solution was prepared by dissolving corn starch in buffer at 20 mg/mL followed by gelatinizing the solution at 100 °C for 2.5 min. The sample was diluted in buffer to appropriate concentrations. Acarbose was prepared in buffer and used as a

positive control. α-Amylase solution (2 U/mL in buffer, 20 μL) or α-glucosidase solution (1×10^{-2} U/mL in buffer, 20 μL) was pre-incubated with inhibitor solution (20 μL) with series of concentrations in a 96-well microplate and kept at 37 °C for 15 min. The reaction was initiated by injecting 60 μL of the gelatinized corn starch solution. The turbidity changes were recorded at 660 nm every 60 sec for 2 h using a microplate absorbance reader (Synergy HT; Biotek Instruments Inc., Winooski, VT, USA). The percentage of inhibition was calculated using Eq. 1.

$$\text{Inhibition}\,(\%) = \frac{AUC_{sample} - AUC_{control}}{AUC_{sample}} \times 100 \quad (1)$$

where AUC_{sample} is the area under the inhibitory curve; and $AUC_{control}$ is the area under the control curve. The IC_{50} can be defined as the concentration of an inhibitor that produces 50% inhibition of enzyme activity under a specified assay condition. It was obtained from interpolation of percentage of inhibition against inhibitor concentration curve.

2.9. *Inhibition kinetics*

The inhibition modes of proanthocyanidins against α-amylase and α-glucosidase were determined through quantifying the amount of released oligosaccharides from soluble starch according to the method developed by Wood and Bhat (1988) with slight modifications. DNSA reagent was prepared by dissolving DNSA (10 g) and sodium potassium tartrate (Rochelle salt, 300 g) in NaOH (2%, 500 mL) solution followed by subsequently diluting to 1 L by deionized water. Sodium phosphate buffer (0.1 M, pH 6.9) was freshly prepared prior to each test and fortified with calcium chloride (40 ppm). The varying substrate concentrations of 1.25, 2.5, 5, and 10 mg/mL were prepared by dissolving corn starch in buffer followed by gelatinizing the solution at 100 °C for 5 min. Serial concentrations of 0, 1, 5, and 10 μg/mL of the proanthocyanidins in buffer were prepared for α-amylase and 0, 50, 75, and 100 μg/mL for α-glucosidase. Similarly, acarbose was dissolved in buffer at the concentrations of 0, 10.74, 15.34, and 21.91 μg/mL for α-amylase and 0, 10, 20, and 31 μg/mL for α-glucosidase as a positive control. Porcine pancreatic α-amylase or rat intestinal α-glucosidase was dissolved in buffer at a fixed concentration of 0.2 mg/mL, respectively. Aliquots of 20 μL of α-amylase or α-glucosidase and *L. alata* extracts (20 μL) were well mixed in a 96-well microplate and pre-incubated at 37 °C for 5 min. The reactions were initiated by adding starch solution (60 μL) in the mixture and incubated for another 5 min at 37 °C. The reactions were then stopped by adding an aliquot of DNSA reagent (100 μL) followed by heating in boiling water for 5 min to develop colour. After cooling down to room temperature in a cold water bath, the absorbance of the mixture was read at 540 nm using the microplate absorbance reader. A negative control was prepared by replacing *L. alata* extracts with buffer (20 μL).

The inhibition mode was graphically determined using the Lineweaver–Burk plot. The inhibition constant (K_i) was calculated through global nonlinear regression of all data sets at once using GraphPad Prism software (Intuitive Software for Science, San Diego, CA, USA). In Lineweaver–Burk double reciprocal plots of inhibited enzyme kinetics, if the fitted lines of inhibited and uninhibited data pass through the same point in the X-axis, the inhibitor is referred to as noncompetitive inhibitor, which binds to both the free enzyme and enzyme-substrate complex. On the other hand, if the lines pass through a common point in the Y-axis, the inhibitor is referred to as competitive inhibitor. Competitive inhibitors bind exclusively to the active site of the free enzyme and consequently preventing the substrates from binding to the free enzyme (Copeland, 2013). Michaelis–Menton equations for mixed noncompetitive inhibition and competitive inhibition (Eqs. 2 and 3) were used for calculation.

$$\frac{1}{\upsilon_0} = \left(1 + \frac{[I]}{\alpha K_i}\right)\frac{1}{V_{max}} + \frac{K_m}{V_{max}[S]}\left(1 + \frac{[I]}{K_i}\right) \quad (2)$$

$$\frac{1}{\upsilon_0} = \frac{[S] + K_m\left(1 + \frac{[I]}{K_i}\right)}{V_{max}[S]} \quad (3)$$

where υ_0 is the initial reaction rate; V_{max} is the maximum reaction rate; $[S]$ is the concentration of substrate; $[I]$ is the inhibitor concentration; K_m is the Michaelis–Menton constant; and α is a factor.

2.10. *Statistical analysis*

All analyses were conducted in at least triplicate, and results were expressed as mean ± standard deviation. Statistical analysis was performed using statistical functions in Excel (Redmond, WA, USA).

3. Results and discussion

3.1. *Inhibitory activities of* L. alata *extracts against α-amylase and α-glucosidase*

Our preliminary studies showed that deionized water had satisfactory extraction efficiency for active compounds in *L. alata* leaves. Investigation on the most appropriate solvent system is crucial, especially for novel feedstocks (Ayoub, de Camargo, & Shahidi, 2016). AEW (acetone : ethanol : deionized water : acetic acid = 40.0 : 40.0 : 19.9 : 0.1, v/v) was normally regarded as an effective solvent for extracting active compounds (Feng et al., 2013). The extraction efficiency of deionized water was found to discriminate better than AEW, i.e. the inhibitory activities of *L. alata* leaves extracted by deionized water against α-amylase and α-glucosidase were 1.3 and 1.5 times higher than that extracted by AEW, respectively (data not shown). Therefore, deionized water was selected as the extraction solvent in this study. It shall be pointed out that some potential inhibitors may need special solvents to be extracted.

As shown in Fig. 1A and B, the *L. alata* extracts could cause an obvious inhibition against α-amylase at a low concentration of 0.85 μg/mL. Increasing the concentration to 1.21 μg/mL could achieve about 80% inhibition. In comparison, the extracts exhibited a much lower inhibitory activity against α-glucosidase (Fig. 1C and D). From the dose response curves (Fig. 1B and D), IC_{50} of the extracts against α-amylase and α-glucosidase were calculated to be 0.77 ± 0.09 and

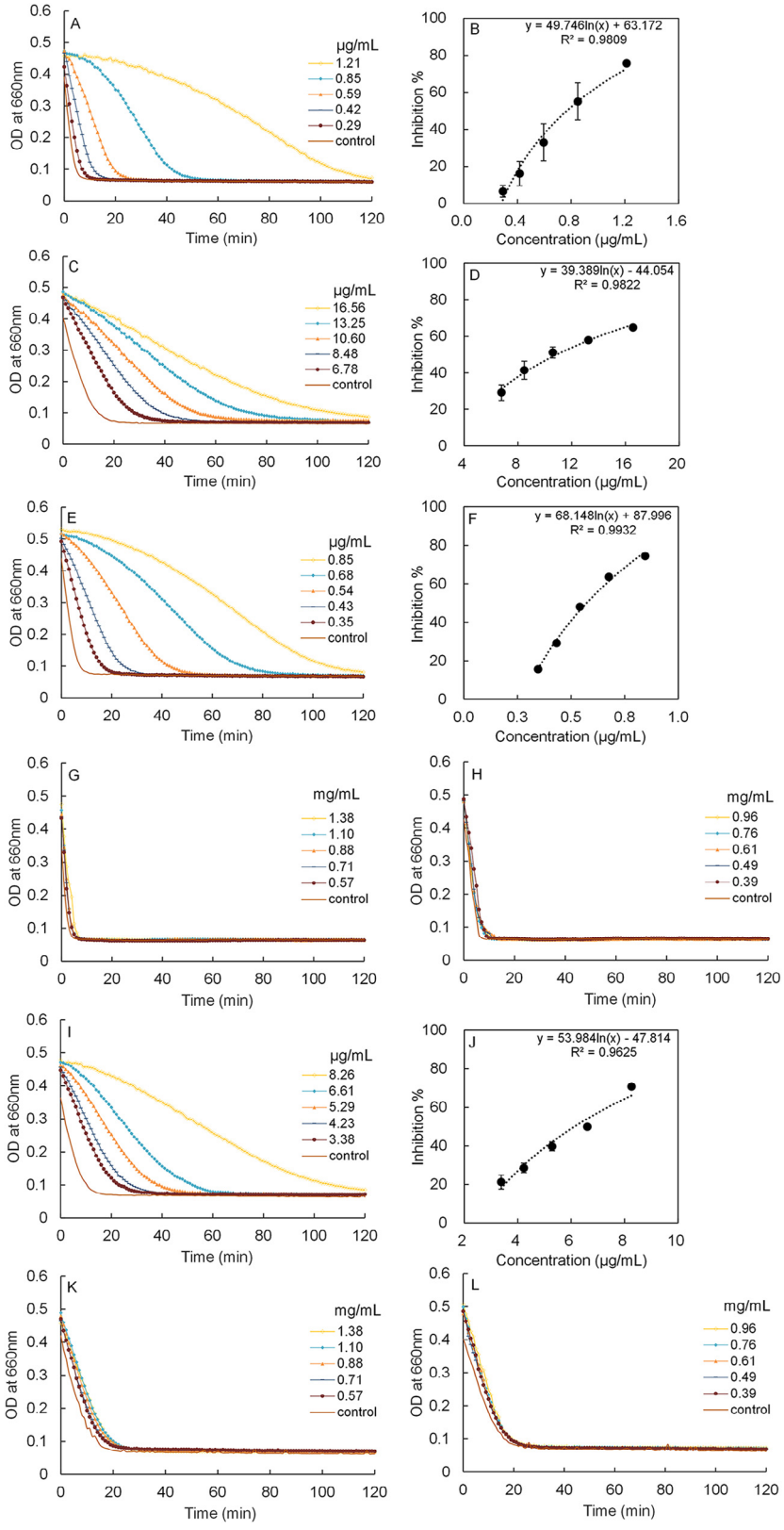

Fig. 1 – The kinetic curve of starch hydrolysis by α-amylase in the presence of different concentrations of (A) aqueous extracts of *L. alata*; (E) proanthocyanidins; (G) thiolysed proanthocyanidins; and (H) the supernatant removal of proanthocyanidins by gelatin binding. Dose response curve of α-amylase inhibitory activity of (B) aqueous extracts of *L. alata* and (F) proanthocyanidins. The kinetic curve of starch hydrolysis by α-glucosidase in the presence of different concentrations of (C) aqueous extracts of *L. alata*; (I) proanthocyanidins; (K) thiolysed proanthocyanidins; and (L) the supernatant removal of proanthocyanidins by gelatin binding. Dose response curve of α-glucosidase inhibitory activity of (D) aqueous extracts of *L. alata* and (J) proanthocyanidins.

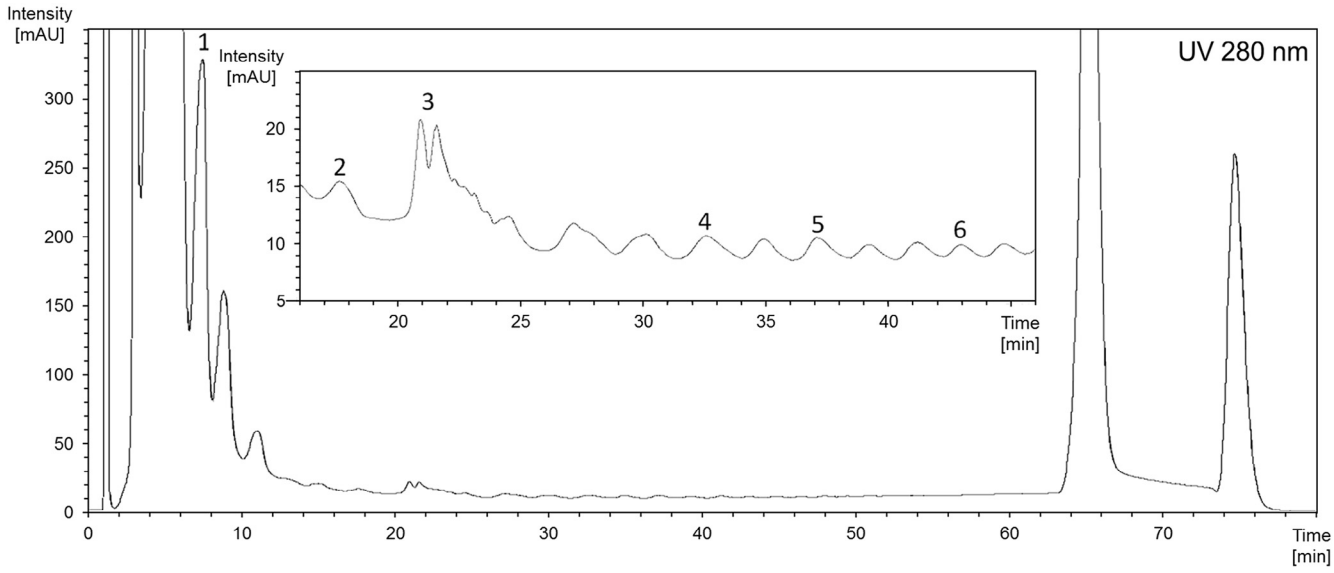

Fig. 2 – HPLC chromatogram of proanthocyanidins of *L. alata* leaves aqueous extracts: (1) dimer B-type, G-C/C-G; (2) trimer B-type, G-$(C)_2$; (3) trimer B-type, $(G)_2$-C; (4) tetramer B-type, $(G)_2$-$(C)_2$; (5) tetramer B-type, G-$(C)_3$; (6) pentamer B-type, G-$(C)_4$(C and G are the abbreviation for (epi)catechin and (epi)gallocatechin, respectively; detector wavelength is set at 280 nm).

10.83 ± 0.67 μg/mL, respectively. As a reference, the IC_{50} of acarbose, measured under the same conditions, were 6.56 (for α-amylase) and 2.12 μg/mL (α-glucosidase), respectively. Therefore, the extract was about 8.5 times more potent than acarbose in inhibiting α-amylase. Acarbose was more active towards α-glucosidase and a stronger inhibitor comparing to the extracts. For convenient comparison, the IC_{50} of the extracts was further expressed as acarbose equivalent (AE). The *L. alata* extracts have inhibitory activities of 13.2 mmol AE/g and 0.3 mmol AE/g for α-amylase and α-glucosidase, respectively. Given the fact, the extracts contain many compounds, and thus it is remarkable that the extracts exhibit stronger inhibitory activity comparing to that acarbose based on equal weight basis.

3.2. *Characterization of proanthocyanidins using LC-ESI/MS*[4]

Proanthocyanidins are notorious for its enzyme inhibitory activity and we suspected it may be responsible in this case too. Therefore, we carried out analysis to determine the proanthocyanidins contents and structural profile in *L. alata* extracts. Indeed, our data suggested the presence of proanthocyanidins in the extracts. The HPLC chromatogram of the oligomeric proanthocyanidins is shown in Fig. 2 and the corresponding MS data are listed in Table 1. The structures were assigned on the basis of the *m/z* of their parent ions and their corresponding daughter ions. (Epi)catechin was expressed as either catechin or epicatechin because mass spectrometry could not distinguish the chirality of C3 on the flavan-3-ols.

Peak 1 was tentatively identified as a B-type dimer of (epi)catechin (C) and (epi)gallocatechin (G) on the basis of MS^2; based on the fragmentation pattern, we can conclude that the linkage is CG. The molecular ion peak $[M-H]^-$ at *m/z* 593 $[306 + 290 - (2-1) \times 2 - 1]^-$ fragmented to give *m/z* 467 $[M-H-126]^-$ (heterocyclic ring fission), *m/z* 425 $[M-H-168]^-$ (retro-Diels–Alder fission), and *m/z* 289 $[M-H-304]^-$ (quinone methide fission) (Bresciani et al., 2015; Wang et al., 2012).

Peak 2 was tentatively identified as a B-type trimer of one (epi)gallocatechin and two (epi)catechins. It had the $[M-H]^-$ at *m/z* 881 $[306 + 290 \times 2 - (3-1) \times 2 - 1]^-$ and fragmented to generate the main MS^2 signal at *m/z* 695 $[M-H-168-18]^-$. The loss of 168 Da and further 18 Da corresponds with cleavage of a retro-Diels–Alder fission of the heterocyclic ring and a molecular of water (Teixeira, Azevedo, Mateus, & de Freitas, 2016).

Table 1 – ESI/MS (anionic mode) of *L. alata* leaf proanthocyanidins.

Peak #	RT (min)	Compound[a]	MW	$[M-H]^-$ (*m/z*)	MS^2 main fragments (*m/z*)
1	7.6	Dimer B-type, G-C/C-G	594	593	467, 425, 289
2	18.2	Trimer B-type, G-(C)2	882	881	695, 543, 525
3	21.3	Trimer B-type, (G)2-C	898	897	711, 593
4	32.7	Tetramer B-type, (G)2-(C)2	1186	1185	1059, 737, 675
5	37.2	Tetramer B-type, G-(C)3	1170	1169	881, 819, 719, 593
6	42.2	Pentamer B-type, G-(C)4	1458	1457	1025, 827, 729

[a] C and G are the abbreviation for (epi)catechin and (epi)gallocatechin, respectively. The stereochemistry of the chiral carbons on the C ring of flavanols units is not defined.

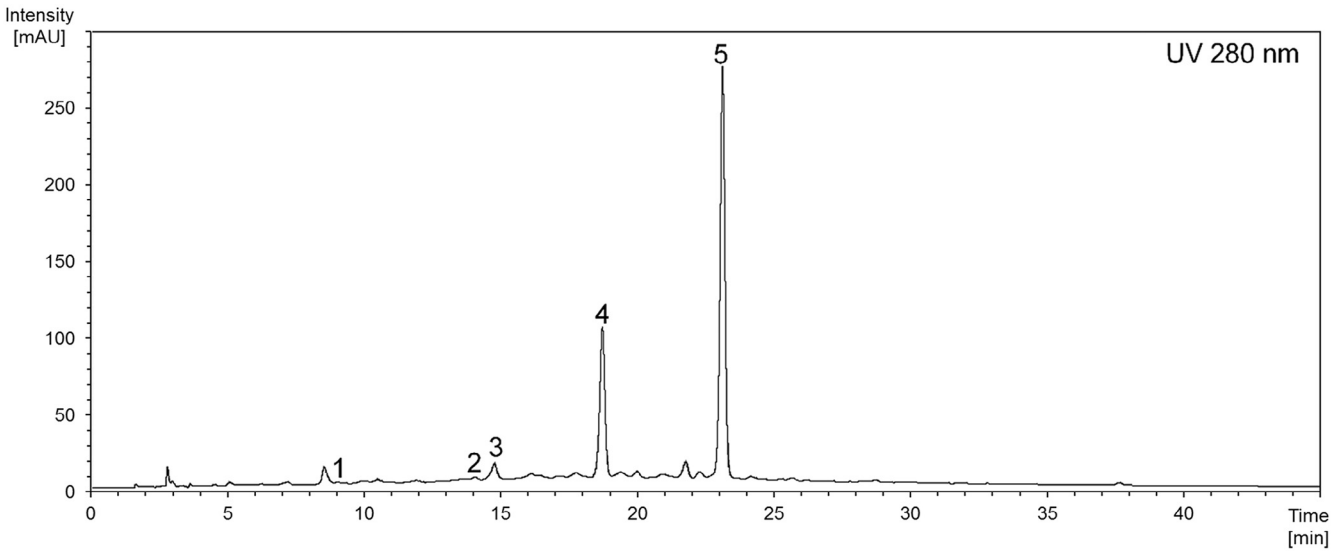

Fig. 3 – HPLC chromatogram of thiolysed products of oligomeric proanthocyanidins by methyl thioglycolate: (1) epigallocatechin; (2) (epi)gallocatechin thioether; (3) epicatechin; (4) (epi)gallocatechin thioether; (5) (epi)catechin thioether (detector wavelength is set at 280 nm).

Peak 3 was tentatively identified as a B-type trimer of two (epi)gallocatechins and one (epi)catechin. It showed the $[M-H]^-$ at *m/z* 897 $[306\times2+290-(3-1)\times2-1]^-$ and fragmented to yield the two main MS^2 signals at *m/z* 711 $[M-H-168-18]^-$ and *m/z* 593 $[M-H-304]^-$. The fragment ion of *m/z* 711 showed the loss of a retro-Diels–Alder fission of the heterocyclic ring and a molecular of water and the signal at *m/z* 593 was due to the loss of (epi)gallocatechin quinone methide (Teixeira et al., 2016).

Peak 4 was tentatively identified as a B-type tetramer of two (epi)gallocatechins and two (epi)catechins. It showed the $[M-H]^-$ at *m/z* 1185 $[306\times2+290\times2-(4-1)\times2-1]^-$ and fragmented to produce the two main MS^2 signals at *m/z* 1059 $[M-H-126]^-$ and *m/z* 737 $[M-H-126-304-18]^-$. The fragment ion of *m/z* 1059 might arise from fission of the heterocyclic rings, while signal at *m/z* 737 might arise from further loss of a (epi)gallocatechin quinone methide and water (Tala et al., 2013).

Peak 5 showed the $[M-H]^-$ at *m/z* 1169 $[306+290\times3-(4-1)\times2-1]^-$ and two MS^2 signals at *m/z* 881 $[M-H-288]^-$ and *m/z* 593 $[M-H-288\times2]^-$. These fragment ions of *m/z* 881 and *m/z* 593 might arise from interflavanyl bond cleavages. These data tentatively led to the assignment of the peak as a B-type tetramer of one (epi)gallocatechin and three (epi)catechins (Es-Safi, Guyot, & Ducrot, 2006; Tala et al., 2013).

Peak 6 showed the $[M-H]^-$ at *m/z* 1457 $[306+290\times4-(5-1)\times2-1]^-$ and ionized to yield the main MS^2 fragments at *m/z* 1025 $[M-H-126-288-18]^-$, which might arise from fission of the heterocyclic rings, cleavage of a interflavanyl bond, and loss of water. Therefore, peak 6 was tentatively identified as a B-type pentamer of one (epi)gallocatechin and four (epi)catechins (Es-Safi et al., 2006).

3.3. *Analysis of thiolysed proanthocyanidins*

Since proanthocyanidins may exist in high molecular weight polymers that cannot be detected by LC-MS, we carried out the thiolysis treatment of the sample. The components in the thiolysed proanthocyanidins solution were analysed by LC-ESI/MS^4 (Fig. 3 and Table 2).

Peak 1 gave an *m/z* 305 (anionic) and *m/z* 307 (cationic), which matched with that of (epi)gallocatechin. Fragments of *m/z* 305 yielded a main fragment ion at *m/z* 179, which was consistent with previously reported data for (epi)gallocatechin (Määttä, Kamal-Eldin, & Törrönen, 2003).

Peaks 2 and 4 both gave an *m/z* value of 409 (anionic) and fitted well to (epi)gallocatechin thioether $[306+106-2-1]^-$. The main daughter ion peak was found at *m/z* 303 $[M-H-106]^-$, which was due to the loss of one methyl thioglycolate molecule. Consistently, Peaks 2 and 4 gave an *m/z* 411 (cationic) and fitted well to (epi)gallocatechin thioether $[306+106-2+1]^+$. The main daughter ion peak of cationic MS^2 was found at *m/z*

Table 2 – ESI/MS of thiolysed products of *L. alata* leaf oligomeric proanthocyanidins.

Peak #	RT (min)	Compound	MW	$[M-H]^-$ (m/z)	Main fragments (m/z)	$[M+H]^+$ (m/z)	Main fragments (m/z)
1	9.3	Epigallocatechin	306	305	179	307	139
2	14.0	(Epi)gallocatechin thioether	410	409	303	411	287
3	14.7	Epicatechin	290	289	245, 205	291	271
4	18.7	(Epi)gallocatechin thioether	410	409	303	411	287
5	23.1	(Epi)catechin thioether	394	393	287	395	289, 271

287 due to the loss of one methyl thioglycolate molecule and one water molecule.

Peak 3 had an *m/z* 289 (anionic) and 291 (cationic), which matched with (epi)catechin. Anionic MS^2 produced fragment ions at *m/z* 245 and 205, which were similar to previous findings (Tsang et al., 2005). This mass spectrum and chromatography with an authentic standard identified peak 3 as epicatechin.

Peak 5 had molecular ion at *m/z* 393 $[M - H]^-$ and is in agreement with (epi)catechin thioether $[290 + 106 - 2 - 1]^-$. The main daughter ion peak of anionic MS^2 gave at *m/z* at 287 $[M - H - 106]^-$, which was the result of the loss of one methyl thioglycolate molecule. In positive ion mode, the molecular ion of peak 5 was found at *m/z* 395. This is in agreement with (epi)catechin thioether $[290 + 106 - 2 + 1]^+$. The main daughter ions peak of cationic MS^2 gave at *m/z* at 289 and 271. The peak at *m/z* 289 $[M + H - 106]^+$ was the result of the loss of one methyl thioglycolate molecule. The peak at *m/z* 271 $[M + H - 106 - 18]^+$ was the result of the loss of one methyl thioglycolate molecule and one water molecule (Chen, Fu, Qin, & Huang, 2009).

From our analysis, the thiolysed solution contains mainly 4β-(carboxymethyl)sulfanyl-(-)-(epi)catechin methyl ester along with significant amounts of 4β-(carboxymethyl)sulfanyl-(-)-(epi)gallocatechin methyl ester, and a trace amount of (epi)catechin and epigallocatechin. This result suggested that there were large amounts of (epi)catechin extension units and (epi)gallocatechin extension units in proanthocyanidins obtained from the leaves of *L. alata*. In addition, the major terminal units in the proanthocyanidins were (epi)catechin and (epi)gallocatechin. Through comparing the peak areas of the individual curves obtained from HPLC chromatogram, the mean degree of polymerization (mDP) of the proanthocyanidins was estimated to be 27 using Eq. 4.

$$\mathrm{mDP} = 1 + \frac{\sum[\text{extension units of thiolated (epi)catechin and thiolated (epi)gallocatechin}]}{\sum[\text{terminal units of epicatechin and epigallocatechin}]} \quad (4)$$

where extension units of thiolated (epi)catechin and thiolated (epi)gallocatechin are the peak areas of thiolated (epi)catechin and thiolated (epi)gallocatechin, respectively, and terminal units of epicatechin and epigallocatechin are the peak areas of epicatechin and epigallocatechin, respectively. Such high degree of polymerization may be responsible for its strong enzyme inhibition activity and good water solubility. In agreement with the thiolysis results, the proton nuclear magnetic resonance (^{1}H NMR) spectrum (Supplementary material Fig. S1) and the MALDI-TOF/MS (Supplementary material Fig. S2) revealed that the proanthocyanidins were mainly oligomers with high degree of polymerization.

3.4. MALDI-TOF/MS analysis of proanthocyanidins

In MALDI-TOF/MS (Fig. S2), a series of peaks arising from the tetramer (*m/z* 1193.2) to pentadecamer (*m/z* 4409.7) were observed. The mass difference between every two adjacent peaks was *m/z* 288 or 304, which coincided with the mass of (epi)catechin or (epi)gallocatechin, respectively. It is worth to notice that the major peak at *m/z* 4409.7 could be assigned as the pentadecamer of three (epi)gallocatechins and twelve (epi)catechins (plus K^+) or the pentadecamer of four (epi)gallocatechins and eleven (epi)catechins (plus Na^+). Since our matrix contained sodium salt of 2,5-dihydroxybenzoic acid, it is more likely that sodium was the charge carrier for the peaks observed in MALDI-TOF/MS.

3.5. Proanthocyanidins as the active compounds against α-amylase and α-glucosidase

After purification by reverse phase HPLC, the inhibitory activities of proanthocyanidins were measured against α-amylase and α-glucosidase (Fig. 1E). They were highly potent as the IC_{50} value was 0.57 ± 0.001 μg/mL (17.8 mmol AE/g) for α-amylase and was 6.12 ± 0.12 μg/mL (0.5 mmol AE/g) for α-glucosidase. Oligomeric or polymeric proanthocyanidins were proven to be effective α-amylase inhibitors (Lee, Cho, Tanaka, & Yokozawa, 2007). However, after thiolysis reaction, the inhibitory activities of the thiolysed proanthocyanidins against α-amylase and α-glucosidase were negligible (Fig. 1G and K). Thus, it might be concluded that oligomeric proanthocyanidins had inhibitory activities and their inhibitory activities were lost once their chemical structures were broken down to monomers. However, acid treatment might result in chemical changes, such as hydrolysis of esters and amides, which deactivated other potentially active compounds. Therefore, we sought an alternative method to confirm that proanthocyanidins were the active compounds without acid treatment.

Besides, our preliminary ^{1}H NMR spectrum (Fig. S1) previously confirmed that proanthocyanidins were the major active compounds in the aqueous extracts. An inspection of whether the proanthocyanidins were the only active compounds was still necessary and conducted through testing the inhibitory activities against α-amylase and α-glucosidase after removing proanthocyanidins. Gelatin, a well-known haze-active protein, could interact with proanthocyanidins to form haze (protein–proanthocyanidins complex) (Siebert et al., 1996; Van Buren, 1978). Addition of gelatin to bind and precipitate the proanthocyanidins greatly diminished the inhibitory activities of the resulting supernatant against α-amylase and α-glucosidase (Fig. 1H and L). This result strongly suggested that proanthocyanidins were the major active compounds.

3.6. Inhibition kinetics

The inhibition modes of proanthocyanidins and acarbose were determined by the Lineweaver–Burk plot as shown in Fig. 4. It is apparent that proanthocyanidins from *L. alata* were mixed noncompetitive inhibitors against α-amylase. Similarly, acarbose also showed mixed noncompetitive inhibition against α-amylase (Fig. 4C). For α-glucosidase, the kinetic data shown in Fig. 4B

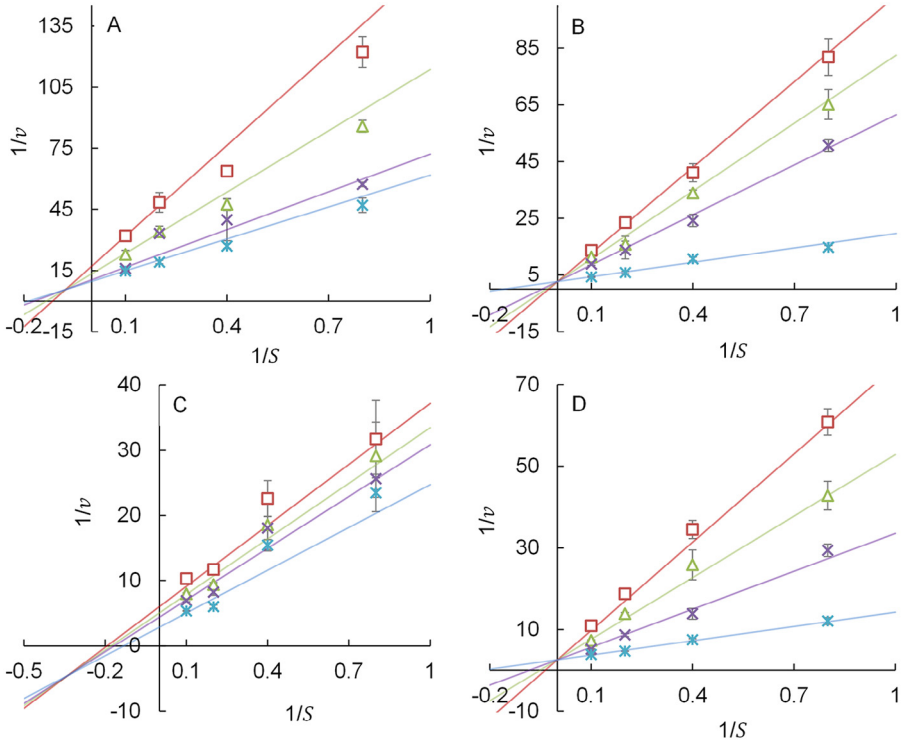

Fig. 4 – (A) Lineweaver–Burk plot of proanthocyanidins against α-amylase. The square, triangle, cross, and asterisk symbols represent proanthocyanidins concentrations of 10, 5, 1, and 0 μg/mL, respectively. (B) Lineweaver–Burk plot of proanthocyanidins against α-glucosidase. The square, triangle, cross, and asterisk symbols represent proanthocyanidins concentrations of 100, 75, 50, and 0 μg/mL, respectively. (C) Lineweaver–Burk plot of acarbose against α-amylase. The square, triangle, cross, and asterisk symbols represent acarbose concentrations of 33.93, 23.76, 16.64, and 0 μM, respectively. (D) Lineweaver–Burk plot of acarbose against α-glucosidase. The square, triangle, cross, and asterisk symbols represent acarbose concentrations of 48.40, 30.98, 15.49, and 0 μM, respectively.

and D are in agreement with competitive inhibitor kinetics. The inhibition constants (K_i), determined from Lineweaver–Burk plot, for proanthocyanidins against α-amylase and α-glucosidase were 5.4 μg/mL and 20.2 μg/mL, respectively. The Michaelis–Menton constants (K_m) for proanthocyanidins against α-amylase and α-glucosidase were 5.4 mg/mL and 6.3 mg/mL.

Tannins are well-known for their non-specific binding with proteins through hydrogen bonding and interaction of the aromatic rings with protein cavity. It is hence remarkable that the proanthocyanidins from *L. alata* exhibited mixed noncompetitive and competitive inhibition against α-amylase and α-glucosidase, respectively. This indicates that the interaction is structure sensitive to the enzymes. Sorghum contains a large proportion of highly polymerized proanthocyanidins and their inhibition mode against α-amylase was found to be noncompetitive (Nguz, Van Gaver, & Huyghebaert, 1998). Similarly, highly polymerized proanthocyanidins in cinnamon bark (Shihabudeen, Priscilla, & Thirumurugan, 2011) were reported as competitive inhibitors against rat intestinal α-glucosidase. Acarbose was classified as a competitive inhibitor against rat intestinal α-glucosidase and a mixed noncompetitive inhibitor against porcine pancreatic α-amylase, which is in agreement with a previous study (Kim et al., 1999). Proanthocyanidins are structurally diverse due to variable monomeric units, chirality, and linkage modes between monomeric units. Therefore, it is necessary to specifically study the proanthocyanidins from different botanical sources in order to fully utilize their health promotion activity. The potent starch hydrolase inhibition activity of proanthocyanidins in *L. alata* leaves warrants further investigation. In particular, we shall understand its performance in mitigating the digestibility of starchy foods *in vivo* and in human. The fact that it is an edible plant makes it attractive for usage in preparing functional foods with low glycaemic index.

Acknowledgement

DH acknowledges the financial support from the National University of Singapore (Suzhou) Research Institute under the grant number R-2012-N-006 and a major grant for Industry-University-Research programme of Jiangsu Province for funding support. YZ thanks China Scholarship Council (CSC) and the National University of Singapore (NUS) for financial support.

Appendix: Supplementary material

Supplementary data to this article can be found online at doi:10.1016/j.jff.2016.06.035.

REFERENCES

Alshikh, N., de Camargo, A. C., & Shahidi, F. (2015). Phenolics of selected lentil cultivars: Antioxidant activities and inhibition of low-density lipoprotein and DNA damage. *Journal of Functional Foods*, *18*(Pt. B), 1022–1038.

Ayoub, M., de Camargo, A. C., & Shahidi, F. (2016). Antioxidants and bioactivities of free, esterified and insoluble-bound phenolics from berry seed meals. *Food Chemistry*, *197*(Pt. A), 221–232.

Bhandari, M. R., Jong-Anurakkun, N., Hong, G., & Kawabata, J. (2008). α-Glucosidase and α-amylase inhibitory activities of Nepalese medicinal herb Pakhanbhed (*Bergenia ciliata*, Haw.). *Food Chemistry*, *106*, 247–252.

Bresciani, L., Calani, L., Cossu, M., Mena, P., Sayegh, M., Ray, S., & Del Rio, D. (2015). (Poly)phenolic characterization of three food supplements containing 36 different fruits, vegetables and berries. *PharmaNutrition*, *3*, 11–19.

Bruyne, T. D., Pieters, L., Deelstra, H., & Vlietinck, A. (1999). Condensed vegetable tannins: Biodiversity in structure and biological activities. *Biochemical Systematics and Ecology*, *27*, 445–459.

Chai, W. M., Wei, M. K., Wang, R., Deng, R. G., Zou, Z. R., & Peng, Y. Y. (2015). Avocado proanthocyanidins as a source of tyrosinase inhibitors: Structure characterization, inhibitory activity, and mechanism. *Journal of Agricultural and Food Chemistry*, *63*, 7381–7387.

Chen, W., Fu, C., Qin, Y., & Huang, D. (2009). One-pot depolymerizative extraction of proanthocyanidins from mangosteen pericarps. *Food Chemistry*, *114*, 874–880.

Clissold, S., & Edwards, C. (1988). Acarbose. *Drugs*, *35*, 214–243.

Copeland, R. A. (2013). Chapter 3. *Evaluation of enzyme inhibitors in drug discovery: A guide for medicinal chemists and pharmacologists*. New York: John Wiley & Sons.

de Camargo, A. C., Regitano-d'Arce, M. A. B., Biasoto, A. C. T., & Shahidi, F. (2016). Enzyme-assisted extraction of phenolics from winemaking by-products: Antioxidant potential and inhibition of alpha-glucosidase and lipase activities. *Food Chemistry*, doi:10.1016/j.foodchem.2016.05.047.

de Camargo, A. C., Regitano-d'Arce, M. A. B., Gallo, C. R., & Shahidi, F. (2015). Gamma-irradiation induced changes in microbiological status, phenolic profile and antioxidant activity of peanut skin. *Journal of Functional Foods*, *12*, 129–143.

Es-Safi, N. E., Guyot, S., & Ducrot, P. H. (2006). NMR, ESI/MS, and MALDI-TOF/MS analysis of pear juice polymeric proanthocyanidins with potent free radical scavenging activity. *Journal of Agricultural and Food Chemistry*, *54*, 6969–6977.

Feng, S., Song, L., Liu, Y., Lai, F., Zuo, G., He, G., Chen, M., & Huang, D. (2013). Hypoglycemic activities of commonly-used traditional Chinese herbs. *The American Journal of Chinese Medicine*, *41*, 849–864.

Fu, C., Loo, A. E. K., Chia, F. P. P., & Huang, D. (2007). Oligomeric proanthocyanidins from mangosteen pericarps. *Journal of Agricultural and Food Chemistry*, *55*, 7689–7694.

Holman, R. R., Cull, C. A., & Turner, R. C. (1999). A randomized double-blind trial of acarbose in type 2 diabetes shows improved glycemic control over 3 years (UK Prospective Diabetes Study 44). *Diabetes Care*, *22*, 960–964.

Kalsum, H. U., & Mirfat, A. (2014). Proximate composition of Malaysian underutilised fruits. *Journal of Tropical Agriculture and Food Science*, *42*, 63–72.

Kim, M. J., Lee, S. B., Lee, H. S., Lee, S. Y., Baek, J. S., Kim, D., Moon, T. W., Robyt, J. F., & Park, K. H. (1999). Comparative study of the inhibition of α-glucosidase, α-amylase, and cyclomaltodextrin glucanosyltransferase by acarbose, isoacarbose, and acarviosine-glucose. *Archives of Biochemistry and Biophysics*, *371*, 277–283.

Lee, Y. A., Cho, E. J., Tanaka, T., & Yokozawa, T. (2007). Inhibitory activities of proanthocyanidins from persimmon against oxidative stress and digestive enzymes related to diabetes. *Journal of Nutritional Science and Vitaminology*, *53*, 287–292.

Lim, T. K. (2013). Lepisanthes alata. In *Edible medicinal and non-medicinal plants* (pp. 39–41). Netherlands: Springer.

Liu, T., Song, L., Wang, H., & Huang, D. (2011). A high-throughput assay for quantification of starch hydrolase inhibition based on turbidity measurement. *Journal of Agricultural and Food Chemistry*, *59*, 9756–9762.

Ma, Y. Y., Zhao, D. G., Zhou, A. Y., Zhang, Y., Du, Z., & Zhang, K. (2015). α-Glucosidase inhibition and antihyperglycemic activity of phenolics from the flowers of *Edgeworthia gardneri*. *Journal of Agricultural and Food Chemistry*, *63*, 8162–8169.

Määttä, K. R., Kamal-Eldin, A., & Törrönen, A. R. (2003). High-performance liquid chromatography (HPLC) analysis of phenolic compounds in berries with diode array and electrospray ionization mass spectrometric (MS) detection: Ribes species. *Journal of Agricultural and Food Chemistry*, *51*, 6736–6744.

Mellor, D. D., Sathyapalan, T., Kilpatrick, E. S., & Atkin, S. L. (2015). Diabetes and chocolate: Friend or foe? *Journal of Agricultural and Food Chemistry*, *63*, 9910–9918.

Morris, C., Fichtel, S. L., & Taylor, A. J. (2011). Impact of calcium on salivary α-amylase activity, starch paste apparent viscosity, and thickness perception. *Chemosensory Perception*, *4*, 116–122.

Murotomi, K., Umeno, A., Yasunaga, M., Shichiri, M., Ishida, N., Koike, T., Matsuo, T., Abe, H., Yoshida, Y., & Nakajima, Y. (2015). Oleuropein-rich diet attenuates hyperglycemia and impaired glucose tolerance in type 2 diabetes model mouse. *Journal of Agricultural and Food Chemistry*, *63*, 6715–6722.

Nakamura, Y., Ogawa, M., Nishide, T., Emi, M., Kosaki, G., Himeno, S., & Matsubara, K. (1984). Sequences of cDNAs for human salivary and pancreatic α-amylases. *Gene*, *28*, 263–270.

Nguz, K., Van Gaver, D., & Huyghebaert, A. (1998). In vitro inhibition of digestive enzymes by sorghum condensed tannins (*Sorghum bicolor* L.(Moench)). *Sciences Des Aliments*, *18*, 507–514.

Nyambe-Silavwe, H., Villa-Rodriguez, J. A., Ifie, I., Holmes, M., Aydin, E., Jensen, J. M., & Williamson, G. (2015). Inhibition of human α-amylase by dietary polyphenols. *Journal of Functional Foods*, *19*, 723–732.

Perricone, N. V. (2010). Enhanced weight loss from a dietary supplement containing standardized phaseolus vulgaris extract in overweight men and women. *Methods : A Companion to Methods in Enzymology*, *12*, 15–22.

Saito, N., Sakai, H., Suzuki, S., Sekihara, H., & Yajima, Y. (1998). Effect of an α-glucosidase inhibitor (voglibose), in combination with sulphonylureas, on glycaemic control in type 2 diabetes patients. *The Journal of International Medical Research*, *26*, 219–232.

Santos-Buelga, C., & Scalbert, A. (2000). Proanthocyanidins and tannin-like compounds-nature, occurrence, dietary intake and effects on nutrition and health. *Journal of the Science of Food and Agriculture*, *80*, 1094–1117.

Shahidi, F., & Ambigaipalan, P. (2015). Phenolics and polyphenolics in foods, beverages and spices: Antioxidant activity and health effects – a review. *Journal of Functional Foods*, *18*, 820–897.

Shahidi, F., & Naczk, M. (2003). Chapter 1. *Phenolics in food and nutraceuticals*. Boca Raton: CRC Press.

Shihabudeen, H. M. S., Priscilla, D. H., & Thirumurugan, K. (2011). Cinnamon extract inhibits a-glucosidase activity and dampens postprandial glucose excursion in diabetic rats. *Nutrition & Metabolism*, *8*, 1–11.

Siebert, K. J., Troukhanova, N. V., & Lynn, P. Y. (1996). Nature of polyphenol-protein interactions. *Journal of Agricultural and Food Chemistry*, *44*, 80–85.

Tala, V. R. S., Candida da Silva, V., Rodrigues, C. M., Nkengfack, A. E., Campaner dos Santos, L., & Vilegas, W. (2013). Characterization of proanthocyanidins from *Parkia biglobosa* (Jacq.) G. Don.(Fabaceae) by flow injection analysis-electrospray ionization ion trap tandem mass spectrometry and liquid chromatography/electrospray ionization mass spectrometry. *Molecules : A Journal of Synthetic Chemistry and Natural Product Chemistry. [electronic resource]*, *18*, 2803–2820.

Teixeira, N., Azevedo, J., Mateus, N., & de Freitas, V. (2016). Proanthocyanidin screening by LC–ESI-MS of Portuguese red wines made with teinturier grapes. *Food Chemistry*, *190*, 300–307.

Toeller, M. (1994). α-Glucosidase inhibitors in diabetes: Efficacy in NIDDM subjects. *European Journal of Clinical Investigation*, *24*, 31–35.

Tsang, C., Auger, C., Mullen, W., Bornet, A., Rouanet, J. M., Crozier, A., & Teissedre, P. L. (2005). The absorption, metabolism and excretion of flavan-3-ols and procyanidins following the ingestion of a grape seed extract by rats. *The British Journal of Nutrition*, *94*, 170–181.

Van Buren, J. (1978). The effect of processing on tannins in apple juice and the role of tannins in haze formation. New York State Agricultural Experiment Station, Special Report, *27*.

Wang, H., Liu, T., Song, L., & Huang, D. (2012). Profiles and α-amylase inhibition activity of proanthocyanidins in unripe *Manilkara zapota* (Chiku). *Journal of Agricultural and Food Chemistry*, *60*, 3098–3104.

Wild, S., Roglic, G., Green, A., Sicree, R., & King, H. (2004). Global prevalence of diabetes estimates for the year 2000 and projections for 2030. *Diabetes Care*, *27*, 1047–1053.

Wood, T. M., & Bhat, K. M. (1988). Methods for measuring cellulase activities. In S. T. Kellogg & W. A. Wood (Eds.), *Methods in enzymology* (pp. 87–112). California: Academic Press.

World Health Organization. World health day 2016: Beat diabetes. (2016). <http://www.who.int/campaigns/world-health-day/2016/en/>.